



Article

Performance Improvement in a Vehicle Suspension System with FLQG and LQG Control Methods

Tayfun Abut ^{1,*}, Enver Salkim ^{2,3} and Andreas Demosthenous ^{3,*}¹ Department of Mechanical Engineering, Mus Alparslan University, 49250 Muş, Türkiye² Department of Electronics and Automation, Mus Alparslan University, 49250 Muş, Türkiye; e.salkim@ucl.ac.uk³ Department of Electronics and Electrical Engineering, University College London (UCL), London WC1E 7JE, UK

* Correspondence: tayfunabut@gmail.com (T.A.); a.demosthenous@ucl.ac.uk (A.D.)

Abstract: This study investigates the effect of active control on a quarter-vehicle suspension system. The car suspension system was modeled using the Lagrange–Euler method. The linear quadratic Gaussian (LQG) and fuzzy linear quadratic Gaussian (FLQG) control methods were designed and used for active control to increase vehicle handling and passenger comfort, with the aim of reducing or eliminating vibrations by performing active control of passive suspension systems using these methods. The optimum values of the coefficients of the points where the membership functions of the LQG and Fuzzy LQG methods touch were obtained using the grey wolf optimization (GWO) algorithm. The success of the control performance rate of the applied methods was compared based on the passive suspension system. In addition, the obtained results were compared with each other and with other studies using the integral time-weighted absolute error (ITAE) performance criterion. The proposed control method yielded significant improvements in vehicle parameters compared with the passive suspension system. Vehicle body movement, vehicle acceleration, suspension deflection, and tire deflection improved by approximately 88.2%, 91.5%, 88%, and 89.4%, respectively. Thus, vehicle driving comfort was significantly enhanced based on the proposed system.



Academic Editors: Md Abdus Samad Kamal and Masakazu Mukai

Received: 8 January 2025

Revised: 26 February 2025

Accepted: 28 February 2025

Published: 10 March 2025

Citation: Abut, T.; Salkim, E.; Demosthenous, A. Performance Improvement in a Vehicle Suspension System with FLQG and LQG Control Methods. *Actuators* **2025**, *14*, 137. <https://doi.org/10.3390/act14030137>

Copyright: © 2025 by the authors. Licensee MDPI, Basel, Switzerland. This article is an open access article distributed under the terms and conditions of the Creative Commons Attribution (CC BY) license (<https://creativecommons.org/licenses/by/4.0/>).

Keywords: active control; linear quadratic Gaussian (LQG); fuzzy linear quadratic Gaussian (FLQG); grey wolf optimization (GWO) algorithm

1. Introduction

The main goal of using suspension systems in vehicles is to increase the driving comfort of the passengers. These systems isolate vehicles from vibrations caused by vehicle speed and road profile. There are various studies on vibration suppression in active suspension systems (ASS) in the automotive industry [1–3]. Information on the design of automobile suspension systems for driving comfort and the control of wheel load changes for frequencies below body structure resonances were studied in [4]. In addition, the optimum active suspension structures for quarter-vehicle models were detailed and various suggestions made in [5]. The first study on this topic applied the H_∞ control method to a complete-vehicle model to analyze shaking and driving performance [6]. Cherry and Jones conducted a study on the control of a suspension system using the fuzzy logic control method [7]. El Madany and Abduljabbar studied quarter-vehicle systems in a simulation environment using the linear quadratic Gaussian (LQG) method [8]. Another study used the genetic algorithm (GA) optimization method and a fuzzy logic controller [9].

Yoshimura et al. [10] applied the sliding mode control algorithm, in which the sliding surface is obtained using linear quadratic control theory, to a quarter-vehicle system in an experimental environment. They showed that the active suspension system improved performance more than the passive suspension system.

The sliding mode neural network inference fuzzy logic control (SMNNFLC) method was proposed by Al-Holou et al. [11]. Their results were compared with sliding mode control (SMC) and sliding mode fuzzy logic control (SMFLC) methods. Active control of the suspension system was achieved with the proportional-integral sliding mode (PISMC) and linear quadratic regulator (LQR) control methods [12]. The methods were compared together with passive suspension. It has been shown that a more robust outcome was obtained using the PISMC method [12]. An experimental study of the linear control of quarter-vehicle systems was conducted by Lauwerys et al. [13]. The control of a quarter car active suspension system with fuzzy logic and proportional-integral-derivative (PID) control methods has been proposed [14] that reduces body acceleration and increases passenger comfort using fuzzy logic control. Fateh and Alavi studied the simulation of the impedance control of an ASS system [15]. The ASS and passive suspension systems were compared, and better performance was observed using the ASS system.

The LQR and PID control methods have been used to control the active suspension system of a quarter car model [16]. This study showed that the displacement performance of the body can be improved using the LQR and PID control scheme. Another study was carried out on the control of the suspension system using intelligent control methods [17]. A simulation of a quarter-vehicle system using the LQR control method was designed by Nagarkar et al. [18]. In this study, the passive system and the LQR control method were compared, and it was observed that driving comfort increased and the LQR method was flexible. On the other hand, a quarter-vehicle suspension system using different road profiles was controlled by the LQR control method [19]. A comprehensive review of the control of vehicle suspension systems was conducted by Aly and Salem [20]. Multi-purpose control of active suspension systems was carried out using the adaptive backstepping control method [21]. To increase driving comfort, this method was applied to a quarter-vehicle system in a simulation environment using the Lyapunov barrier function. The quarter-car suspension system was controlled by the PID control method, and the outcome was compared with the passive state [22]. It was shown that driving comfort and road holding increased.

An experimental study was conducted by Tang et al. [23]. The study was developed using a state observer-based Takagi-Sugeno fuzzy controller (SOTSFC) for a semi-active quarter-car suspension system equipped with a magnetorheological (MR) damper. The results of this method were compared to the Skyhook controller. Yu et al. [24] carried out an experimental study on a quarter car based on a series of active variable geometry suspensions. The method achieved a success rate of up to 41% without degrading suspension deflection. Khazaie et al. [25] carried out a study on a suspension model that prevents quarter-vehicle suspension systems from losing contact with the road. Nagarkar and his research group [26] simulated the control of a quarter-vehicle system using PID and LQR control methods. Multi-objective optimization was performed using a genetic algorithm. It was observed that driving comfort increased.

Na et al. [27] implemented adaptive finite-time fuzzy control of nonlinear active suspension systems with input delay. The systems were designed, and these methods were applied to a quarter-vehicle system in Carsim and MATLAB simulation environments. The results were calculated and recorded accordingly, showing promising performance. Song and Wang proposed an incremental model predictive control (MPC) method for active suspension systems using an experimental test [28]. The results of this study were

compared with two traditional control methods. Na et al. [29] performed active suspension control of a quarter-vehicle system based on experimental tests. Unlike existing techniques, this study did not use any function methods such as neural networks (NNs) or fuzzy logic systems (FLSs). Active control of quarter and half vehicle suspension systems has been achieved using PID, PID-LQR, and LQR Fuzzy PID control methods [30]. When these methods are compared, it is shown that the Fuzzy-PID controller reduces vibration of car body displacement, car body acceleration, and wheel deflection in the rear and front suspension systems. However, it was shown that using the Fuzzy PID control method produced an unsatisfactory ride and poor handling in the rear suspension system.

Shalabi et al. [31] conducted an experimental study using neuro-fuzzy sound control of a quarter-vehicle system with an air spring suspension system. In this study, a pressure controller based on the FLC methods was used. The air volume was designed and simulated using ANFIS. It has been shown that increasing the total air volume led to a reduction in the transmitted acceleration to the mass. The active control of the quarter-car system was simulated using fuzzy PID and LQR control methods [32]. Although it has been stated that both methods improve the operation of the system, using the LQR method resulted in a better performance compared to the PID method. Shafiei investigated the impact of the PID method on a quarter-vehicle model using the Ziegler–Nichols method through the control system designer application [33].

Adaptive harmonic control of a quarter-vehicle suspension system was examined by Nichiștea and Unguritu [34]. The PI controller, H_∞ controller, and model predictive controllers were simulated. It was observed that a better performance was obtained using the adaptive harmonic control method. The experimental verification of the control of the active suspension system in a quarter-vehicle system was studied by Huang et al. [35]. A reliable, efficient, and simple control was presented and verified for a quarter-vehicle active suspension system equipped with an electro-hydraulic actuator. The approximation-free control (AFC) method was used in the study. The applicability, effectiveness, and generality of the AFC method were investigated for different road conditions based on the various experimental tests. The results were compared with the AFC method with back-stepping and PID controllers. It was found that using the AFC method resulted in improved performance based on all parameters, including the suspension displacements and acceleration responses with regard to the safety of the suspension system and the comfort of the passengers.

Abut and Salkim investigated the active control of a quarter-vehicle suspension system using the PSO-based fuzzy LQR control method [36]. The graphical and numerical variations results were based on the LQR, and the PSO-based control methods were compared. Additionally, the results were compared based on the passive system and other research. It was shown that the performance of the suspension system increased compared to the passive system based on the integral time-weighted absolute error (ITAE) performance criterion. It was also observed that the suspension performance significantly increased compared to the passive system. Vehicle body movement, vehicle acceleration, suspension deflection, and tire deflection were improved by 84.2%, 90%, 84.5%, and 86.7%, respectively. It was shown that road handling and driving comfort increased compared to state-of-the-art systems. A neural network algorithm based on reinforcement learning was used to optimize the LQR controller and applied to a quarter-vehicle system [37]. It was reported that user comfort increased by 67% and 14% compared to the passive system and the non-optimized LQR, respectively.

In this study, the active control of a quarter-vehicle suspension system was modeled using the Lagrange–Euler method. LQG and FLQG control methods were designed and used for active control to increase vehicle handling and passenger comfort. The study

aims to reduce or eliminate unwanted vibrations by performing active control of passive suspension systems using the recommended methods. The optimum values of the coefficients of the points where the membership functions of the LQG and Fuzzy LQG methods touch were obtained using the grey wolf optimization (GWO) algorithm. The success of the control performance of the applied methods based on the passive suspension system was compared. The results were compared with each other and with other work based on the ITAE performance criterion and RMSE performance criteria. It was shown that using the proposed control method resulted in significant improvements compared to the passive suspension system. Car body movement, vehicle acceleration, suspension deflection, and tire deflection were improved by 88.2%, 91.5%, 88%, and 89.4%, respectively. In addition, vehicle driving comfort was significantly improved.

This study investigates active control methods that aim to reduce vibrations in vehicle suspension systems. It has been observed that conventional passive suspension systems cannot reduce vibrations effectively enough and fail to improve ride comfort. To fill this gap, LQG (linear quadratic Gaussian) and FLQG (fuzzy linear quadratic Gaussian) control methods are used for active control, and the GWO (grey wolf optimization) algorithm is applied to determine the optimum control parameters. As a result, significant performance improvements were obtained compared to the passive suspension system. The effectiveness of the active control methods has been more clearly demonstrated by comparing the passive system with existing studies in literature and significant improvements in vehicle parameters have been achieved.

The contributions of this study are as follows:

- a By utilizing the grey wolf optimization (GWO) algorithm, this study determines the optimal weights of the points where the membership functions of the fuzzy LQG control method intersect. The application of this control method to the active suspension system enables the quarter-car suspension to make its own decisions to optimally determine the critical Q and R parameters in system control.
- b The second contribution is the comparison of the LQG and fuzzy LQG control methods with each other and the comparison of their results with the those of passive suspension system.
- c The third contribution is enabling the comparison of the effectiveness of the control methods using performance indices, both relative to each other and to other existing research in the field.

The main contribution of this study is to combine the self-determination capability of the fuzzy logic control method with the advantages of the LQG control method, which is one of the optimal control methods, and to introduce it into the literature on the control of ASSs.

The rest of the paper is organized as follows: Section 2 presents the modeling of the suspension system. Section 3 describes the design of the LQG, Kalman filter, and GWO-based fuzzy LQG control methods. The results of the methods used are presented, compared, and discussed in Section 4. Concluding remarks and future directions are provided in Section 5.

2. Modeling of the Suspension System

The model of the quarter-vehicle system with two degrees of freedom was obtained using the Lagrange–Euler method, as shown in Figure 1. The model was symmetrically divided into four parts and the vertical vibration movement and the pitching and rolling movements of the chassis and wheel were not considered. The model equations are shown below.

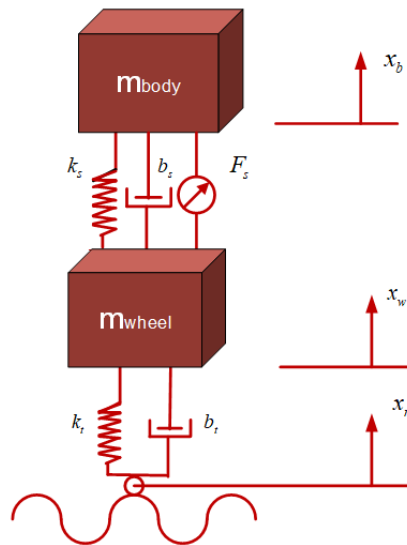


Figure 1. The quarter car model of the active suspension.

Here, m_b indicates the mass of one-quarter of the vehicle body, m_w is the mass of the wheel assembly, k_s is the spring coefficient of the suspension system, b_s is the damping coefficient of the suspension system, k_t the spring coefficient of the tire, and b_t the damper coefficient of the tire. In addition, while the state variables show the displacement (x_w), movements of the body (x_b), and the wheel assembly, the input variables x_r show the road roughness (distortion) and F_s shows the control force applied by the active element applied between the body and the wheel.

$$m_b \ddot{x}_b + b_s (\dot{x}_b - \dot{x}_w) + k_s (x_b - x_w) - F_s = 0 \quad (1)$$

$$m_w \ddot{x}_w + b_t (\dot{x}_w - \dot{x}_r) + k_t (x_w - x_r) - b_s (\dot{x}_b - \dot{x}_w) - k_s (x_b - x_w) - F_s = 0 \quad (2)$$

$$\ddot{x}_b = -\frac{1}{m_b} (b_s (\dot{x}_b - \dot{x}_w) + k_s (x_b - x_w) - F_s) \quad (3)$$

$$\ddot{x}_w = -\frac{1}{m_w} (b_t (\dot{x}_w - \dot{x}_r) + k_t (x_w - x_r) - b_s (\dot{x}_b - \dot{x}_w) - k_s (x_b - x_w) - F_s) \quad (4)$$

$$x_1 = x_b; x_2 = x_w; x_3 = \dot{x}_b; x_4 = \dot{x}_w \quad (5)$$

$$\dot{x}_1 = x_2$$

$$\dot{x}_2 = -\frac{1}{m_b} (b_s (x_3 - x_4) + k_s (x_1 - x_2) - F_s)$$

$$\dot{x}_3 = x_4$$

$$\dot{x}_4 = -\frac{1}{m_w} (b_t (x_4 - \dot{x}_r) + k_t (x_2 - x_r) - b_s (x_3 - x_4) - k_s (x_1 - x_2) - F_s) \quad (6)$$

The dynamic model of the linear moving system is formed as follows in the form of state-space form $\dot{x} = Ax + Bu$.

$$\begin{bmatrix} \dot{x}_1 \\ \dot{x}_2 \\ \dot{x}_3 \\ \dot{x}_4 \end{bmatrix} = \begin{bmatrix} 0 & 1 & 0 & 0 \\ -\frac{k_s}{m_b} & -\frac{b_s}{m_b} & \frac{k_s}{m_b} & \frac{b_s}{m_b} \\ 0 & 0 & 0 & 1 \\ \frac{k_s}{m_w} & \frac{b_s}{m_w} & -\frac{k_s - k_t}{m_w} & -\frac{b_s}{m_w} \end{bmatrix} \begin{bmatrix} x_1 \\ x_2 \\ x_3 \\ x_4 \end{bmatrix} + \begin{bmatrix} 0 & 0 \\ 0 & \frac{1}{m_b} \\ 0 & 0 \\ \frac{k_t}{m_w} & -\frac{1}{m_w} \end{bmatrix} \begin{bmatrix} F_s \\ x_r \end{bmatrix} \quad (7)$$

$$y = \begin{bmatrix} 1 & 0 & 0 & 0 \\ 1 & 0 & -1 & 0 \\ -\frac{k_s}{m_b} & -\frac{b_s}{m_b} & \frac{k_s}{m_b} & \frac{b_s}{m_b} \end{bmatrix} \begin{bmatrix} x_1 \\ x_2 \\ x_3 \\ x_4 \end{bmatrix} + \begin{bmatrix} 0 & 0 \\ 0 & 0 \\ 0 & \frac{1}{m_b} \end{bmatrix} \quad (8)$$

Equation (9) shows the transfer function to the dynamics of the actuator used in the active suspension system.

$$H_{act}(s) = \frac{1}{1/60s + 1} \quad (9)$$

A 5 cm-high road bump was obtained using Equation (10).

$$r(t) = 0.025 * [1 - \cos(8\pi t)] \quad (10)$$

In this study, the measurement of body acceleration \ddot{x}_b was used as feedback and control of the quarter-vehicle active suspension system was given.

3. System Controller Designs

The purpose of the controller designs is to increase vehicle handling and passenger comfort. It aims to reduce vibrations and design a robust system using the recommended control methods in active suspension systems. The main goal is to obtain minimal error values by increasing vehicle handling and passenger comfort. The linear quadratic Gaussian (LQG) and the fuzzy LQG methods were used to control the quarter-vehicle suspension system. These methods are detailed as follows: The LQG control method is one of the optimal control methods. It is a method where the LQR and a Kalman filter are used together [38,39]. Thus, information will first be given about the LQR control method. The most important problem of optimal control methods is to determine the optimal control law that minimizes the performance index, which is determined under various economic and safety constraints.

The LQR control method is a control method based on the state-space model of the system [40,41]. The main goal of this method is to obtain the control signals that cause physical constraints or lead to an excessive (maximizing or minimizing) performance criterion or cost function. The system is controlled with the LQR control method, the input is $u = -K * x$, and K and u indicate the feedback control input and the states of the system, respectively. The state-space equations are used to select a control input to minimize the cost function.

$$J = \frac{1}{2} \int_0^t (x^T(t)Qx + u^T Ru) dt \quad (11)$$

The control system aims to minimize the integral of the quadratic performance index. Q and R are weight matrices, Q is a positive semi-definite symmetric matrix, and R is a positive definite matrix ($Q \geq 0$, $R > 0$). The control vector is represented by u and x shows the states of the system. Equation (11) is a quadratic concerning both $x(t)$ and $u(t)$. The optimum feedback input (K) is calculated using Equation (12).

$$K = R^{-1}B^T P \quad (12)$$

B and P represent the input matrix and positive definite, respectively, and the value of the P matrix was obtained using the Riccati equation. A represents the state matrix.

$$A^T P + PA - PBR^{-1}B^T P + Q = 0 \quad (13)$$

The LQG control method is beneficial as it solves the disadvantage of the LQR control method (requires sensors for each situation) by replacing it with an observer Kalman

filter [42,43]. This eliminates the deficiency that arises due to the inability to measure all states of the system and is very useful as it reduces the cost. However, it does not guarantee the system’s robustness against uncertainties in environmental conditions. The Kalman filter is used to estimate the system’s state based on the system output. It estimates the states of the systems from the input and output information of the systems and can optimally filter measurement and process noises with known covariances of the noises [44–46]. This filter is used to minimize the covariance matrix of the error due to the Gaussian measurement or process noise. Figure 2 shows the block diagram of the linear quadratic Gaussian (LQG) control method.

$$\dot{x} = Ax + Bu + w_d \tag{14}$$

$$y = Cx + Du + w_n \tag{15}$$

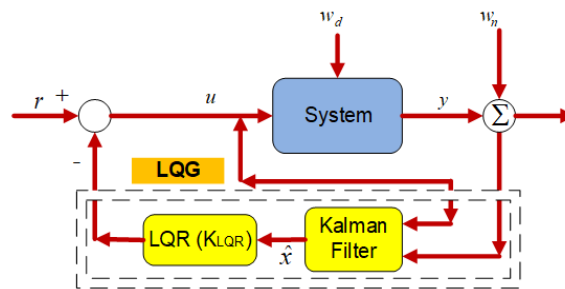


Figure 2. Block diagram of the LQG control method.

In this diagram, w_d represents the process noise given to the random system, and w_n represents the measurement noise. Using known inputs u and measurement y , a Kalman filter is used to estimate the state vector and output vector. The equations of the Kalman estimator are given below (from (16) to (18)):

$$\dot{\hat{x}} = A\hat{x} + Bu + L(y - \hat{y}) \tag{16}$$

$$\hat{y} = C\hat{x} \tag{17}$$

$$PA + A^T P - PC^T R^{-1} CP + Q = 0 \tag{18}$$

where \hat{x} is the predicted x value, Q must be positive definite, R must be positive semidefinite, and the system must be observable. Process noise is expressed as $w \sim N(0, Q)$ and measurement noise as $v \sim N(0, Q)$. Q is the input covariance matrix and R is the output covariance matrix. The algebraic constant P , which minimizes the cost function, is obtained from the Ricatti equation. The filter constant (L) was calculated using the Ricatti equation and the below equation:

$$L = R^{-1} C^T P \tag{19}$$

LQG controllers can be used in both linear time-invariant and linear time-varying systems. This control method has many uses since it can also be applied to nonlinear systems [46].

$$\dot{\hat{x}} = (A - LC - BK)\hat{x} + Ly \tag{20}$$

$$u = -K\hat{x} \tag{21}$$

Fuzzy LQR control is a method in which the advantageous aspects of the LQR and fuzzy control methods are used together [46,47]. The matrices containing the Q and R parameters, which are of critical importance in the LQR control method, are obtained by the fuzzy logic method. This leads the LQR method to have a dynamic structure. This increases the performance of the method (fuzzy LQR) due to changing conditions. The fuzzy LQR

controller calculates $K = [k1, k2, k3]$ state feedback gain values by applying the rules of the fuzzy logic controller, which uses the error and its derivative as input. The boundary values of the membership functions are calculated with the grey wolf optimization (GWO) algorithm [48,49], which is one of the herd-based optimization algorithms.

The grey wolf optimization (GWO) algorithm is a contemporary herd-based meta-heuristic optimization technique that is widely used in various studies. Herd-based methods are preferred due to their ability to provide global optimum solutions, as well as their speed, simplicity, and deterministic nature. The GWO algorithm was first proposed by Mirjalilli et al. [48]. It has gained popularity because of its efficiency in finding global optimum solutions, offering superior performance compared to other optimization techniques [48,49]. This success is particularly evident in solving various problems found in the literature. The core idea behind the GWO algorithm is inspired by the social structure and hunting strategies of grey wolves in the wild. Grey wolves employ three fundamental hunting behaviors: encircling, hunting, and attacking prey. Additionally, they have a hierarchical social structure divided into four main classes: Alpha (α), Beta (β), Delta (δ), and Omega (ω).

Alpha (α) wolves: These are the leaders of the pack, positioned at the top of the hierarchy. They make all major decisions regarding the pack's activities, including when to sleep and walk, and how to manage the hunting process. Their role is crucial in maintaining order and discipline within the pack.

Beta (β) wolves: Positioned below the Alpha wolves, Betas are the second-in-command and serve as the main support for the Alpha in decision-making processes. They help guide the pack and often assist with leadership tasks.

Delta (δ) wolves: Delta wolves are situated in the third tier of the pyramid. Their responsibilities include ensuring the pack's survival, maintaining the pack's social balance, and securing the food supply.

Omega (ω) wolves: The lowest-ranking wolves in the hierarchy, Omega wolves must follow the orders of the higher classes. They are typically tasked with supporting the pack in catching prey.

The GWO algorithm's ability to find global optima stems from its powerful search capability, which is modeled on the hunting behaviors of grey wolves. The algorithm starts with random search and calculates the suitability value of each wolf based on the cost function. In the process of generating candidate solutions, the best solutions are structured according to the hierarchical order, from Alpha at the top to Omega at the bottom. Mirjalilli et al. [48] defined the encircling behavior of the wolves with the following equations:

$$\vec{D} = \left| \vec{D} \cdot \vec{X}_p(t) - \vec{X}(t) \right| \quad (22)$$

$$\vec{X}(t+1) = \vec{X}_p(t) - \vec{A} \cdot \vec{D} \quad (23)$$

In this context, t represents the instantaneous iteration, while A and C are coefficient vectors. X_p denotes the position vector of the prey, and X represents the position vector of a grey wolf. The coefficient vectors A and C are calculated using the Equations (24) and (25).

$$\vec{A} = 2\vec{\alpha} \cdot \vec{r}_1 - \vec{\alpha} \quad (24)$$

$$\vec{C} = 2\vec{r}_2 \quad (25)$$

In this algorithm, r_1 and r_2 are random vectors within the range $[0, 1]$. The parameter α represents a coefficient that decreases linearly from 2 to 0 throughout the iterations. The top three solutions obtained during the search process are recorded, and the positions of

the other wolves are updated based on the positions of the best search agents. These top three solutions are assigned to the Alpha (α), Beta (β), and Delta (δ) wolves, respectively. The Omega (ω) wolves must update their positions according to these top three wolves.

$$\vec{D}_\alpha = \left| \vec{C}_1 \cdot \vec{X}_\alpha - \vec{X} \right| \quad (26)$$

$$\vec{D}_\beta = \left| \vec{C}_2 \cdot \vec{X}_\beta - \vec{X} \right| \quad (27)$$

$$\vec{D}_\delta = \left| \vec{C}_3 \cdot \vec{X}_\delta - \vec{X} \right| \quad (28)$$

$$\vec{X}_1 = \vec{X}_\alpha - \vec{A}_1(\vec{D}_\alpha) \quad (29)$$

$$\vec{X}_2 = \vec{X}_\beta - \vec{A}_2(\vec{D}_\beta) \quad (30)$$

$$\vec{X}_3 = \vec{X}_\delta - \vec{A}_3(\vec{D}_\delta) \quad (31)$$

$$\vec{X}(t+1) = \frac{\vec{X}_1 + \vec{X}_2 + \vec{X}_3}{3} \quad (32)$$

X_α , X_β , and X_δ represent the positions of the Alpha, Beta, and Delta wolves, respectively. X denotes the current position of a wolf, while $X(t+1)$ indicates the updated position of the prey. The top three wolves are continually updated with each iteration. C_1 , C_2 , and C_3 are randomly generated vectors, and A_1 , A_2 , and A_3 represent the calculated coefficient vectors. In summary, the GWO algorithm primarily searches based on the locations of the Alpha, Beta, and Delta wolves. These wolves separate to search for prey, but they converge when attacking the prey. To mathematically model this behavior, the A parameter is assigned random values greater than 1 or less than 1. This variability supports the exploration process, which is key for the global search capabilities of the GWO algorithm.

Step 1: First, start the wolf population ($X_i(i = 1, 2, 3, \dots, n)$) and enter the parameters α , A , and C .

Step 2: Calculate the appropriate position of each wolf in the population and select the three wolves with the best positions in them as α , β , and δ .

Step 3: Update the positions of other wolves in the pack (Equations (25)–(31)).

Step 4: Update α , A and C parameters (Equations (24) and (25)).

Step 5: Calculate the appropriateness of the positions of all wolves in the pack.

Step 6: Update the positions of X_α , X_β , and X_δ (alpha, beta, and delta) wolves.

Step 7: When the maximum number of iterations is reached, the global optimum α position is obtained. Otherwise, step 2 should be repeated to update the parameters.

Mean square error (MSE) was used as the objective function to minimize error values (for the GWO algorithm). The Mamdani method and triangle-type membership functions were used. The flowchart steps of the GWO algorithm applied to the fuzzy LQG control method are given below.

Steps of the Flowchart:

Step 1. Define the Fuzzy LQG Model: First, create the overall design of the fuzzy logic controller and the LQG control structure. This determines the basic structure of the controlled system.

Step 2. Define Membership Functions: Determine the linguistic terms to be used in the system (e.g., “low”, “medium”, “high”) and create the membership functions. These functions define the classifications in which the control inputs will be evaluated.

Step 3. Start Grey Wolf Optimization Algorithm: Initialize the population (wolves) of the GWO algorithm. Each wolf represents a combination of membership functions.

Step 4. Define Fitness Function: Define the fitness function for the GWO algorithm. This function measures the performance of the control system (e.g., minimizing the sum of error squares).

Step 5. Calculate Fitness Values: Test the solution of each wolf and calculate the fitness function. This shows how good each solution (coefficient) is.

Step 6. Find the Best Solution: Identify the Alpha (best) wolf and the helper wolves (Beta, Delta). These wolves are the leaders that will lead to the better solution.

Step 7. Update Pack Movement: The wolves move through the solution space, guided by the leaders. They follow the pack behavior when updating their position (coefficients).

Step 8. Check Iterations: Repeat the steps until the set maximum number of iterations is reached. During iterations, the wolves' solutions improve.

Step 9. Determine the Optimal Coefficients: At the end of the iterations, determine the best solution (optimal coefficients).

Step 10. Use the Optimal Coefficients in the Fuzzy LQG Model: Apply the optimal membership function coefficients obtained with the GWO algorithm to the fuzzy LQG control system.

Step 11. Evaluate the Results: Evaluate the performance of the system. Observe how successful the control system is. If the performance is insufficient, you can adjust the model and repeat the process.

Mean square error (MSE) was used as the objective function to minimize error values (for the GWO algorithm). The Mamdani method and triangle-type membership functions were used. Membership functions (e, \dot{e} ve F) and the rule table for the fuzzy LQR method are shown below in Figure 3, Tables 1 and 2. For the GWO algorithm, the population of wolves was selected as 40 and the maximum number of iterations was selected as 30. It was observed that the optimum values were obtained.

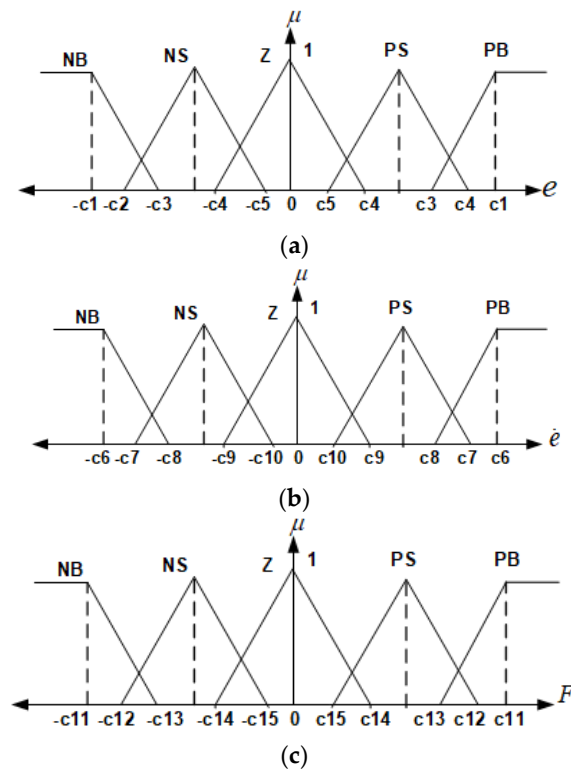


Figure 3. The membership functions of (a) the input e , (b) the input \dot{e} , and (c) the output F .

Table 1. The limit values of FLQR membership functions.

c_1	c_2	c_3	c_4	c_5	c_6	c_7	c_8
1.8	1.4	0.83	0.42	0.23	1.63	1.34	0.92
c_9	c_{10}	c_{11}	c_{12}	c_{13}	c_{14}	c_{15}	
0.64	0.36	1.42	1.1	0.74	0.33	0.18	

Table 2. FLQR rule table.

F	NB	NS	Z	PS	PB
NB	NB	NS	PB	NB	PS
NS	NS	NB	NS	PS	Z
Z	Z	NB	NB	PB	PB
PS	NB	NS	PS	PB	PS
PB	Z	Z	PB	PS	PB

The limit values and rule table of membership functions in the fuzzy LQR method are shown in Tables 1 and 2. The variables of the FLQR method, e, \dot{e}, F , indicate error, error change, and strength, respectively. NB, NS, Z, PS, and PB represent negative big, negative small, zero, positive small, and positive big, respectively, as shown in Table 2. Figure 4 shows the block diagram of the fuzzy LQG control method.

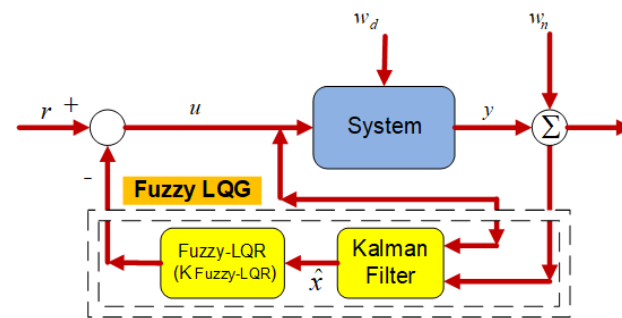


Figure 4. The block diagram of the fuzzy LQG control method.

4. Simulation Results and Discussion

The control algorithms based on fuzzy LQG methods using LQG and GWO were designed and implemented for a quarter car suspension system. The results were calculated accordingly, and the variations were saved in tables and graphs, as will be detailed in this section. The main purpose of controlling the vehicle suspension system is to minimize the disruptive effects caused by road entry that affect passenger comfort.

The physical parameters of the quarter-vehicle suspension system are $m_b = 300$ kg, $m_w = 60$ kg, $k_s = 16,000$ N/m, $b_s = 1000$ Ns/m, $k_t = 190,000$ N/m, and $b_t = 1000$ Ns/m. The initial value of the position of the vehicle suspension system is $x = 0$ m. The system simulation time was 2.5 s. The road entrance is a mound, and it is about 5 cm high, as shown in Figure 5.

The results for the fuzzy LQG based on LQG and GWO for passive and active control of the suspension system are shown in Figure 6. The vehicle’s body motion and body acceleration are the factors that influence passenger comfort. The impact of these parameters based on the passive state is shown in Figures 6 and 7. These results were obtained based on fuzzy LQG control methods using LQG and GWO.

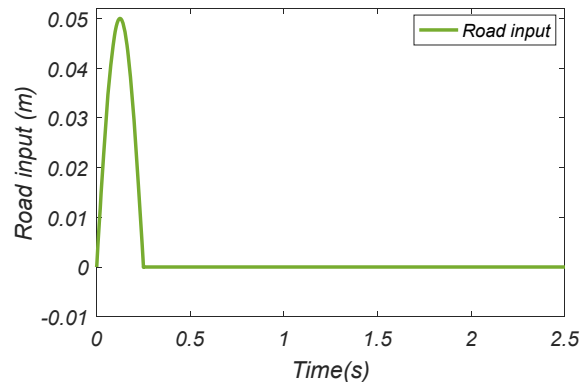


Figure 5. The road input.

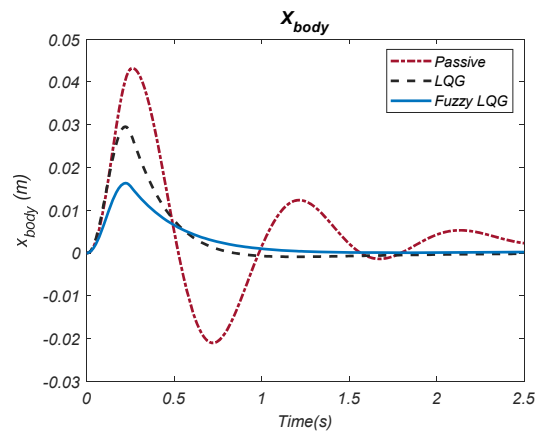


Figure 6. The change in motion of the body.

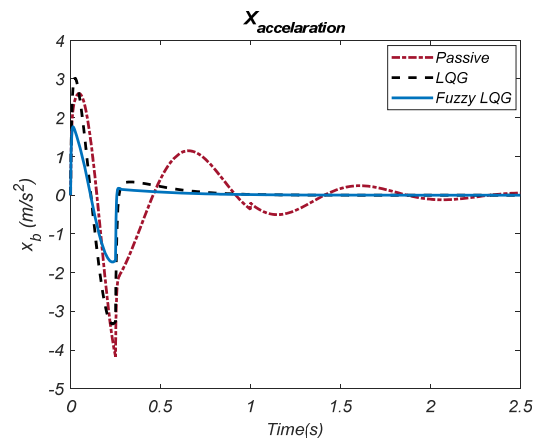


Figure 7. The change in body acceleration.

The results of the vertical displacement movement of the vehicle body, displayed in Figure 6, show that the vibration amplitude and settling time are significantly reduced based on all control methods compared to the passive suspension system. Relatively lower vibration amplitude values are obtained when the fuzzy LQG method based on GWO is used (between 0.016~0 m) compared to the LQG (0.029~0.001 m) method. As shown in Figure 7, the performance of damping the acceleration amplitudes is relatively better when the fuzzy LQG control type based on GWO is used compared to the LQG method. While the range of the acceleration is ± 1.75 m/s² for the fuzzy LQG control type based on GWO, this is about (3~(-3.2) m) for the LQG method. The results for the suspension deflection and tire deflection based on the applied control methods are shown in Figures 8 and 9, respectively.

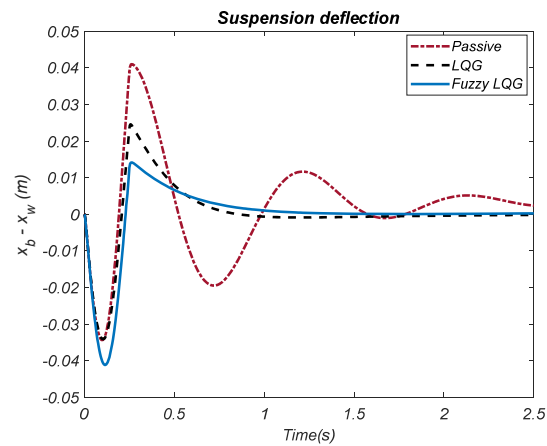


Figure 8. The change in suspension deflection.

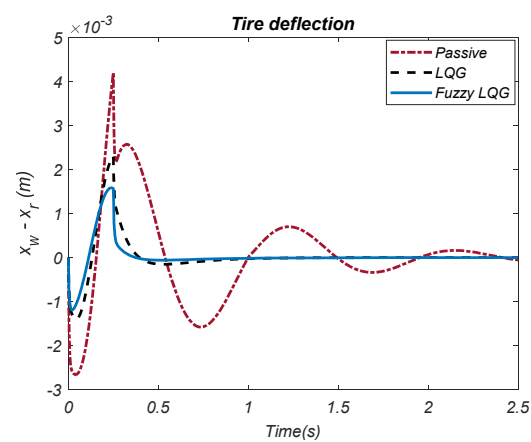


Figure 9. The change in tire deflection.

This shows that the fuzzy LQG control method is more effective in reducing vibrations, resulting in less oscillation and greater system stability. These results help assess how effectively the applied control methods manage the deflections in both the suspension and tires. Proper deflection control is crucial for maintaining the vehicle's stability and handling, as excessive deflections can lead to discomfort or reduced control over the vehicle, especially in challenging driving conditions.

The results of the suspension contraction in Figure 8 show that the contraction amplitudes of the fuzzy LQG control type based on GWO are lower than the LQG control method. The contraction amplitude varies between 0.014~0 m for the fuzzy LQG control type based on GWO. This range for the LQG method is about 0.024~0 m. It is shown in Figure 9 that the tire deflection amplitude is relatively lower for the fuzzy LQG control type based on GWO compared to the LQG control method. The tire deflection amplitude ranges for the fuzzy LQG control type based on GWO is about $-0.0011\sim 0.0015$ m. This range is approximately $-0.001\sim 0.0021$ m for the LQG control method. The force graph used in active control is shown in Figure 10.

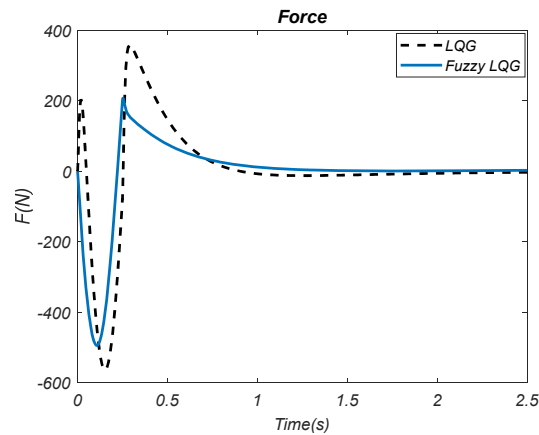


Figure 10. The change in force.

The low amount of force used by a controller to reduce vibrations makes the method advantageous. The change in force is shown in Figure 10. It is shown that the variation in the force is approximately within the range of $-490\sim 205$ N based on the GWO-based fuzzy LQG control method. This variation is approximately $-556\sim 352$ N when the LQG control type was used. Overall, the fuzzy LQG type controller provides better control with less force when all the results in the figures are considered.

$$ITAE = \int_0^t t e dt \quad (33)$$

The parameters of vehicle body motion, vehicle acceleration, suspension deflection, tire deflection, and the force required to be applied were calculated using (33) for the methods used in this study, as shown in Table 3. The results were compared using the ITAE performance index. Similarly, the methods were compared using the RMSE criterion given in Equation (34), and the results are given in Table 4.

$$RMSE = \sqrt{\frac{1}{n} \sum_i e_i^2} \quad (34)$$

Table 3. The change in motion of the body.

Performance Criteria (ITAE)	Passive	LQG	Fuzzy LQG
Body travel (X_{body}) (m)	0.01914	0.0039	0.0023
Body acceleration (\ddot{X}_{body}) (m/s^2)	0.75410	0.1355	0.0604
Suspension deflection ($X_{body} - X_{wheel}$) (m)	0.01801	0.0037	0.0022
Tire deflection ($X_{wheel} - X_{road}$) (m)	0.00113	0.00026	0.0012
Actuator (F) (N)	-	65.45	55.27

The car body motion's lowest error based on the ITAE performance criteria is highlighted in bold in Table 3. The lowest error was obtained using the fuzzy LQG method compared to the LQG control method. The error rate is about 0.0023 m for the fuzzy LQG method and about 0.0039 m for the LQG method. When the acceleration error results are compared based on the used control methods, as shown in Table 3, the lowest value is recorded for the fuzzy LQG when using the GWO control method compared to the LQG method. While the acceleration error is about 0.0604 m/s^2 for the fuzzy LQG using GWO, it is 0.1355 m/s^2 when using the LQG method.

Table 4. The comparisons of applied control methods using performance criteria.

Performance Criteria (RMSE)	Passive	LQG	Fuzzy LQG
Body travel (X_{body}) (m)	0.04914	0.0142	0.0094
Body acceleration (\ddot{X}_{body}) (m/s^2)	0.94870	0.2746	0.0961
Suspension deflection ($X_{body} - X_{wheel}$) (m)	0.09242	0.0237	0.0185
Tire deflection ($X_{wheel} - X_{road}$) (m)	0.00874	0.00845	0.0345
Actuator (F) (N)	-	293.83	121.74

According to the suspension clearance error results, the lowest error performance was obtained using the GWO-based fuzzy LQG method with 0.0022 m, while this value is 0.0039 m for the LQG method. In addition, the results for the tire deviation error show that using the GWO-based fuzzy LQG method resulted in a lower error of about 0.00012 m. It is shown that the tire deviation error is about 0.00026 when the LQG method is used. When the force errors are compared using control methods, it is shown that the lowest force error value of 55.27 N is obtained using the GWO-based fuzzy LQR control method. However, this value is 65.45 N for the LQG method, as shown in Table 3. The percentage improvement performance of the control methods based on the passive system was calculated using (35), and the results are shown in Figure 11. The results are highlighted in blue and yellow for the fuzzy LQG and LQG methods, respectively.

$$Improvement(\%) = \left| \frac{passive - active}{passive} \right| * 100 \tag{35}$$

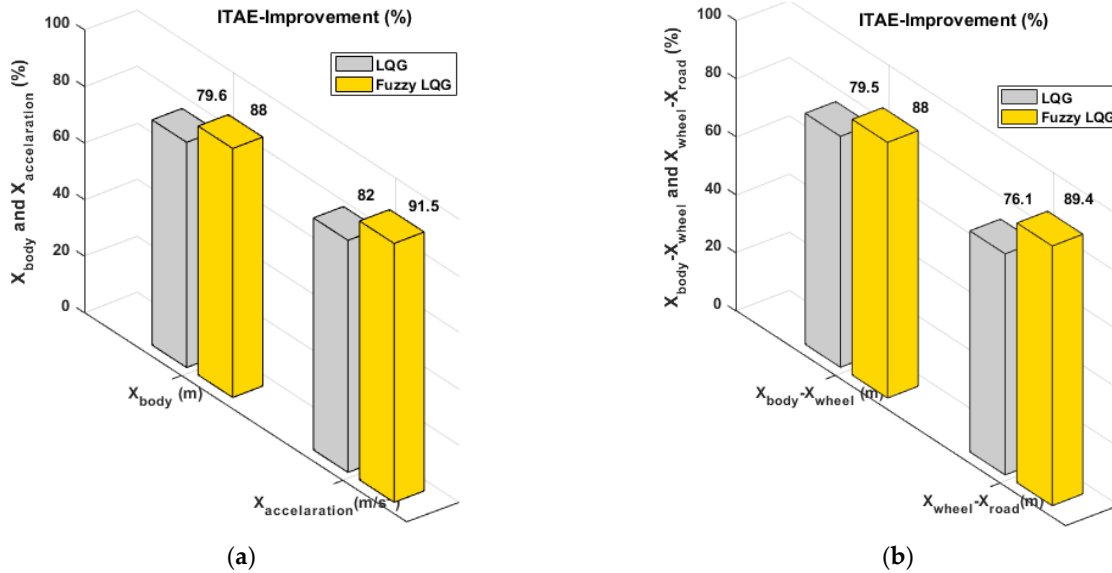


Figure 11. The percentage performance comparisons of the (a) X body position and X body acceleration and the (b) suspension and tire deflection.

As the car body motion’s lowest error results based on the RMSE performance criteria highlighted in bold in Table 4, the lowest error was obtained using the fuzzy LQG method compared to the LQG control method. The error rate was about 0.0142 m for the fuzzy LQG method and 0.0094 m for the LQG method. When the acceleration error results were compared based on the used control methods, shown in Table 4, the lowest value was recorded for the fuzzy LQG using the GWO control method compared to the LQG method.

While the acceleration error was about 0.2746 m/s^2 for the fuzzy LQG using GWO, it was 0.0961 m/s^2 when using the LQG method.

According to the suspension clearance error results, the lowest error performance was obtained using the GWO-based fuzzy LQG method with 0.0185 m , and this value was 0.0237 m for the LQG method. In addition, the results based on the tire deviation error show that using the GWO-based fuzzy LQG method resulted in a lower error of about 0.0345 m . It is shown that the tire deviation error is about 0.00845 when the LQG method is used. When the force errors are compared using control methods, it is shown that the lowest force error result is obtained using the GWO-based fuzzy LQR control method, which is 121.74 N . However, this value is 293.83 N for the LQG method, as shown in Table 4.

It is shown that the fuzzy LQG control method exhibits superior performance based on all parameters compared to the LQG method. The performance of all parameters is significantly increased compared to the passive system. When the fuzzy LQG control method is used, the of vehicle body movement performance increases by 79.6% while vehicle acceleration increases by 82% , and these improvements are 79.5% and 76.1% for the suspension deflection and tire deflection, respectively. Table 5 compares the proposed fuzzy LQG method with other works.

Table 5. Comparison of the proposed fuzzy LQG method with existing methods.

Performance Criteria (ITAE)	Fuzzy LQG	PSO-Based Fuzzy LQR [36]	Harmonic [34]	H-Infinity [34]	MPC [34]
Body travel (X_{body}) (m)	0.0023	0.00302	0.0039	0.0071	0.0041
Body acceleration (\ddot{X}_{body}) (m/s^2)	0.0604	0.07545	0.1683	0.1588	0.1252
Suspension deflection ($X_{body} - X_{wheel}$) (m)	0.0022	0.00280	0.0044	0.0072	0.0046
Tire deflection ($X_{wheel} - X_{road}$) (m)	0.0012	0.00015	-	-	-
Actuator (F) (N)	55.27	59.29	64	95.5	80.7

As shown in Table 5, the error values for vehicle body movement, vehicle acceleration, suspension deflection, and tire deflection are compared based on the PSO-based fuzzy LQR, harmonic, MPC, H-infinity control, and fuzzy LQG methods. Bold characters are used to highlight the lowest error performance values. It is seen that the results for the proposed fuzzy LQG control method are superior to all other existing methods.

In summary, the fuzzy LQG method (based on GWO) performs significantly better than the LQG method in reducing vibration amplitudes and acceleration fluctuations, making the vehicle more stable and responsive. Both methods outperform the passive suspension system, demonstrating that the active control strategies lead to better vehicle performance in terms of minimizing vibrations and improving ride comfort. Additionally, the results for suspension deflection and tire deflection further support the effectiveness of the applied control methods in enhancing overall vehicle dynamics.

The limitations of this study can be expressed as follows: In the model used in the study, variables such as environmental factors, road conditions, and driving style in real-world conditions are not included. Therefore, simulation results may not be equally effective in the real world. The performance of GWO may change, especially when the parameters are nonlinear or the system's complexity increases. This study only presents valid results for the model given in the paper. The fuzzy LQG method used in the study is optimized under certain conditions. However, its ability to continuously adapt to changing

conditions in the system (e.g., speed, load, road surface changes) may be limited. Applying the method in an experimental setting can overcome many of these limitations.

5. Conclusions

This study investigated the performance of a quarter-vehicle model using two different control methods. The various parameters of the quarter car were investigated, and the results were recorded. It was shown that desired vehicle handling and passenger comfort were achieved using the proposed control method. Active control of the quarter-vehicle system was carried out using LQG and fuzzy LQG methods. The designed controllers were implemented in the computer environment and the results were compared using the ITAE criterion and RMSE criteria. Additionally, the performance of the controllers was compared to the passive suspension system. The results showed that the performance of the proposed method (fuzzy LQG control method) led to a significant improvement in the movement of the vehicle body in the suspension system, vehicle acceleration, suspension deflection, and tire deflection compared to the passive system. The results also showed a significant improvement in vehicle driving comfort. In future works, it may be feasible to apply the proposed method to half- and full-vehicle models. In addition, the relationship between bumper height and pedestrian injuries [50] can be examined when modeling the quarter-vehicle system.

Author Contributions: Writing—original draft, T.A.; Writing—review & editing, T.A., E.S. and A.D.; Visualization, T.A. and E.S.; Supervision, A.D. All authors have read and agreed to the published version of the manuscript.

Funding: This research was funded by University College London (UCL).

Data Availability Statement: All data generated or analyzed during this study are included in the article.

Conflicts of Interest: The authors declared no potential conflicts of interest with respect to the research, authorship, and/or publication of this article.

Nomenclature

m_b	Mass of a quarter car body
m_w	Mass of the wheel assembly
k_s	Spring coefficient of the suspension system
b_s	Damper coefficient of the suspension system
k_t	Spring coefficient of the tire
b_t	Damper coefficient of the tire
x_b	Body travel
\ddot{x}_b	Body acceleration
x_w	Displacement of the wheel assembly
x_r	The road roughness (distortion)
$x_b - x_w$	Suspension deflection
$x_w - x_r$	Tire deflection
F_s	Actuator control force
ASS	Active Suspension System
LQG	Linear Quadratic Gaussian
LQR	Linear Quadratic Regulator
PSO	Particle Swarm Optimization Algorithm
Fuzzy – LQG	Fuzzy Linear Quadratic Gaussian

References

1. Du, H.; Li, W.; Zhang, N. Integrated seat and suspension control for a quarter car with driver model. *IEEE Trans. Veh. Technol.* **2012**, *61*, 3893–3908. [[CrossRef](#)]
2. Yan, L.; Chen, J.; Duan, C.; Zhao, C.; Yang, R. A Vibration Control Method Using MRASSA for 1/4 Semi-Active Suspension Systems. *Electronics* **2023**, *12*, 1778. [[CrossRef](#)]
3. Abbas, S.B.; Youn, I. Optimal Control of a Semi-Active Suspension System Collaborated by an Active Aerodynamic Surface Based on a Quarter-Car Model. *Electronics* **2024**, *13*, 3884. [[CrossRef](#)]
4. Sharp, R.S.; Crolla, D.A. Road vehicle suspension system design—A review. *Veh. Syst. Dyn.* **1987**, *16*, 167–192. [[CrossRef](#)]
5. Hrovat, D. Optimal active suspension structures for quarter-car vehicle models. *Automatica* **1990**, *26*, 845–860. [[CrossRef](#)]
6. Yamashita, M.; Fujimori, K.; Hayakawa, K.; Kimura, H. Application of H_{∞} control to active suspension systems. *Automatica* **1994**, *30*, 1717–1729. [[CrossRef](#)]
7. Cherry, A.; Jones, R. Fuzzy logic control of an automotive suspension system. *IEE Proc.-Control Theory Appl.* **1995**, *142*, 149–160. [[CrossRef](#)]
8. ElMadany, M.M.; Abduljabbar, Z.S. Linear quadratic gaussian control of a quarter-car suspension. *Veh. Syst. Dyn.* **1999**, *32*, 479–497. [[CrossRef](#)]
9. D’amato, F.J.; Viassolo, D.E. Fuzzy control for active suspensions. *Mechatronics* **2000**, *10*, 897–920. [[CrossRef](#)]
10. Yoshimura, T.; Kume, A.; Kurimoto, M.; Hino, J. Construction of an active suspension system of a quarter car model using the concept of sliding mode control. *J. Sound Vib.* **2001**, *239*, 187–199. [[CrossRef](#)]
11. Al-Holou, N.; Lahdhiri, T.; Joo, D.S.; Weaver, J.; Al-Abbas, F. Sliding mode neural network inference fuzzy logic control for active suspension systems. *IEEE Trans. Fuzzy Syst.* **2002**, *10*, 234–246. [[CrossRef](#)]
12. Sam, Y.M.; Osman, J.H.; Ghani, M.A. A class of proportional-integral sliding mode control with application to active suspension system. *Syst. Control Lett.* **2004**, *51*, 217–223. [[CrossRef](#)]
13. Lauwerys, C.; Swevers, J.; Sas, P. Robust linear control of an active suspension on a quarter car test-rig. *Control Eng. Pract.* **2005**, *13*, 577–586. [[CrossRef](#)]
14. Salem, M.M.; Aly, A.A. Fuzzy control of a quarter-car suspension system. *Int. J. Comput. Inf. Eng.* **2009**, *3*, 1276–1281.
15. Fateh, M.M.; Alavi, S.S. Impedance control of an active suspension system. *Mechatronics* **2009**, *19*, 134–140. [[CrossRef](#)]
16. Lin, J.; Lian, R.-J. Intelligent control of active suspension systems. *IEEE Trans. Ind. Electron.* **2010**, *58*, 618–628. [[CrossRef](#)]
17. Darus, R.; Enzai, N.I. Modeling and control active suspension system for a quarter car model. In Proceedings of the International Conference on Science and Social Research (CSSR 2010), Kuala Lumpur, Malaysia, 5–7 December 2010; pp. 1203–1206.
18. Nagarkar, M.; Vikhe, G.; Borole, K.; Nandedkar, V. Active control of quarter car suspension system using linear quadratic regulator. *Int. J. Automot. Mech. Eng.* **2011**, *3*, 364–372. [[CrossRef](#)]
19. Agharkakli, A.; Sabet, G.S.; Barouz, A. Simulation and analysis of passive and active suspension system using quarter car model for different road profile. *Int. J. Eng. Trends Technol.* **2012**, *3*, 636–644.
20. Aly, A.A.; Salem, F.A. Vehicle suspension systems control: A review. *Int. J. Control Autom. Syst.* **2013**, *2*, 46–54.
21. Sun, W.; Pan, H.; Zhang, Y.; Gao, H. Multi-objective control for uncertain nonlinear active suspension systems. *Mechatronics* **2014**, *24*, 318–327. [[CrossRef](#)]
22. Ahmed, A.E.-N.S.; Ali, A.S.; Ghazaly, N.M.; El-Jaber, G.T.A. PID controller of active suspension system for a quarter car model. *Int. J. Adv. Eng. Technol.* **2015**, *8*, 899–909.
23. Tang, X.; Du, H.; Sun, S.; Ning, D.; Xing, Z.; Li, W. Takagi–Sugeno fuzzy control for semi-active vehicle suspension with a magnetorheological damper and experimental validation. *IEEE/ASME Trans. Mechatron.* **2016**, *22*, 291–300. [[CrossRef](#)]
24. Yu, M.; Arana, C.; Evangelou, S.A.; Dini, D. Quarter-car experimental study for series active variable geometry suspension. *IEEE Trans. Control Syst. Technol.* **2017**, *27*, 743–759. [[CrossRef](#)]
25. Khazaie, A.; Hussaini, N.; Marzbani, H.; Jazar, R.N. Quarter car suspension model with provision for loss of contact with the road. In *Nonlinear Approaches in Engineering Applications: Energy, Vibrations, and Modern Applications*; Springer: Cham, Switzerland, 2018; pp. 167–208.
26. Nagarkar, M.; Bhalerao, Y.; Patil, G.V.; Patil, Z. Multi-objective optimization of nonlinear quarter car suspension system—PID and LQR control. *Procedia Manuf.* **2018**, *20*, 420–427. [[CrossRef](#)]
27. Na, J.; Huang, Y.; Wu, X.; Su, S.-F.; Li, G. Adaptive finite-time fuzzy control of nonlinear active suspension systems with input delay. *IEEE Trans. Cybern.* **2019**, *50*, 2639–2650. [[CrossRef](#)]
28. Song, S.; Wang, J. Incremental model predictive control of active suspensions with estimated road preview information from a lead vehicle. *J. Dyn. Syst. Meas. Control* **2020**, *142*, 121004. [[CrossRef](#)]
29. Na, J.; Huang, Y.; Wu, X.; Liu, Y.-J.; Li, Y.; Li, G. Active suspension control of quarter-car system with experimental validation. *IEEE Trans. Syst. Man Cybern. Syst.* **2022**, *52*, 4714–4726. [[CrossRef](#)]
30. Munawwarah, S.; Yakub, F. Control analysis of vehicle ride comfort through integrated control devices on the quarter and half car active suspension systems. *Proc. Inst. Mech. Eng. Part D J. Automob. Eng.* **2020**, *235*, 1256–1268. [[CrossRef](#)]

31. Shalabi, M.E.; Elbab, A.M.R.F.; El-Hussieny, H.; Abouelsoud, A.A. Neuro-fuzzy volume control for quarter car air-spring suspension system. *IEEE Access* **2021**, *9*, 77611–77623. [[CrossRef](#)]
32. Ahmed, A.A. Quarter car model optimization of active suspension system using fuzzy PID and linear quadratic regulator controllers. *Glob. J. Eng. Technol. Adv.* **2021**, *6*, 88–97. [[CrossRef](#)]
33. Shafiei, B. A Review on PID control system simulation of the active suspension system of a quarter car model while hitting road bumps. *J. Inst. Eng. (India) Ser. C* **2022**, *103*, 1001–1011. [[CrossRef](#)]
34. Nichiștea, T.C.; Unguritu, M.G. Design and comparisons of adaptive harmonic control for a quarter-car active suspension. *Proc. Inst. Mech. Eng. Part D J. Automob. Eng.* **2022**, *236*, 343–352. [[CrossRef](#)]
35. Huang, Y.; Na, J.; Wu, X.; Gao, G. Approximation-free control for vehicle active suspensions with hydraulic actuator. *IEEE Trans. Ind. Electron.* **2018**, *65*, 7258–7267. [[CrossRef](#)]
36. Abut, T.; Salkim, E. Control of quarter-car active suspension system based on optimized fuzzy linear quadratic regulator control method. *Appl. Sci.* **2023**, *13*, 8802. [[CrossRef](#)]
37. Kozek, M.; Smoter, A.; Lalik, K. Neural-assisted synthesis of a linear quadratic controller for applications in active suspension systems of wheeled vehicles. *Energies* **2023**, *16*, 1677. [[CrossRef](#)]
38. Athans, M. The role and use of the stochastic linear-quadratic-Gaussian problem in control system design. *IEEE Trans. Autom. Control* **1971**, *16*, 529–552. [[CrossRef](#)]
39. Bernstein, D.S.; Haddad, W.M. LQG control with an H_∞ performance bound: A riccati equation approach. In Proceedings of the 1988 American Control Conference, Atlanta, GA, USA, 15–17 June 1988; pp. 796–802.
40. Anderson, B.D.; Moore, J.B. *Optimal Control: Linear Quadratic Methods*; Courier Corporation: Chelmsford, MA, USA, 2007.
41. Abut, T. Modeling and optimal control of a DC motor. *Int. J. Eng. Trends Technol.* **2016**, *32*, 146–150. [[CrossRef](#)]
42. Mohinder, S.G.; Angus, P.A. *Kalman Filtering: Theory and Practice Using Matlab*; Wiley: New York, NY, USA, 2001.
43. Grewal, M.S.; Andrews, A.P. *Kalman Filtering: Theory and Practice with MATLAB*; John Wiley & Sons: New York, NY, USA, 2014.
44. Banerjee, R.; Pal, A.; Sinha, A.; Mukherjee, D. Stabilization of Cart-Pole System-A Linear Quadratic Gaussian Control and Robust H-infinity Control Design and Comparative Approach. In Proceedings of the International Conference on Advances in Electrical and Computer Technologies, Coimbatore, India, 28–29 October 2020; Springer Nature Singapore: Singapore, 2020; pp. 831–845.
45. Adeli, M.; Zarabadipour, H.; Zarabadi, S.H.; Shoorehdeli, M.A. Anti-swing control for a double-pendulum-type overhead crane via parallel distributed fuzzy LQR controller combined with genetic fuzzy rule set selection. In Proceedings of the 2011 IEEE International Conference on Control System, Computing and Engineering, Penang, Malaysia, 25–27 November 2011; pp. 306–311.
46. Collins, E.; Selekw, M. A fuzzy logic approach to LQG design with variance constraints. *IEEE Trans. Control Syst. Technol.* **2002**, *10*, 32–42. [[CrossRef](#)]
47. Zadeh, L.A. Fuzzy logic. *Computer* **1988**, *21*, 83–93. [[CrossRef](#)]
48. Mirjalili, S.; Mirjalili, S.M.; Lewis, A. Grey wolf optimizer. *Adv. Eng. Softw.* **2014**, *69*, 46–61. [[CrossRef](#)]
49. Faris, H.; Aljarah, I.; Al-Betar, M.A.; Mirjalili, S. Grey wolf optimizer: A review of recent variants and applications. *Neural Comput. Appl.* **2017**, *30*, 413–435. [[CrossRef](#)]
50. Agarwal, A.; Batista, R.C.; Gurung, A. Analyzing the impact of bumper height on pedestrian injuries using explicit dynamics. In *Smart Electric and Hybrid Vehicles*; CRC Press: Boca Raton, FL, USA, 2024; pp. 57–89.

Disclaimer/Publisher’s Note: The statements, opinions and data contained in all publications are solely those of the individual author(s) and contributor(s) and not of MDPI and/or the editor(s). MDPI and/or the editor(s) disclaim responsibility for any injury to people or property resulting from any ideas, methods, instructions or products referred to in the content.